ISSN 1063-7834, Physics of the Solid State, 2011, Vol. 53, No. 6, pp. 1202–1211. © Pleiades Publishing, Ltd., 2011.
Original Russian Text © E.I. Pogorel'tsev, E.V. Bogdanov, M.S. Molokeev, V.N. Voronov, L.I. Isaenko, S.A. Zhurkov, N.M. Laptash, M.V. Gorev, I.N. Flerov, 2011, published in Fizika Tverdogo Tela, 2011, Vol. 53, No. 6, pp. 1136–1145.

DIELECTRICS

Thermodynamic Properties and Structure of Oxyfluorides $Rb_2KMoO_3F_3$ and $K_2NaMoO_3F_3$

E. I. Pogorel'tsev[a,*], E. V. Bogdanov[b], M. S. Molokeev[b], V. N. Voronov[b], L. I. Isaenko[c], S. A. Zhurkov[c], N. M. Laptash[d], M. V. Gorev[a,b], and I. N. Flerov[a,b,]**

[a] *Institute of Engineering Physics and Radioelectronics, Siberian Federal University, pr. Svobodnyi 79, Krasnoyarsk, 660041 Russia*

* *e-mail: pepel@iph.krasn.ru*

** *e-mail: flerov@iph.krasn.ru*

[b] *Kirensky Institute of Physics, Siberian Branch, Russian Academy of Sciences, Akademgorodok, Krasnoyarsk, 660036 Russia*

[c] *Sobolev Institute of Geology and Mineralogy, Siberian Branch, Russian Academy of Sciences, pr. Akademika Koptyuga 3, Novosibirsk, 630090 Russia*

[d] *Institute of Chemistry, Far Eastern Branch, Russian Academy of Sciences, ul. Stoletiya Vladivostoka 159, Vladivostok, 690022 Russia*

Received November 22, 2010

Abstract—According to the results of calorimetric and structural studies, the $Fm\bar{3}m$ phase in $K_2NaMoO_3F_3$ remains stable at least to 100 K. No ferroelectric transformation assumed earlier has been revealed in a series of $Rb_2KMoO_3F_3$ samples prepared using various technologies. Only a phase transition of nonferroelectric origin has been observed near 195 K, and its thermodynamic characteristics have been determined. An analysis of the stability of the cubic structure of molybdenum fluorine–oxygen elpasolites–cryolites has been performed in the framework of the hypothesis on strengths of interatomic bonds. The barocaloric effect in $Rb_2KMoO_3F_3$ has been estimated.

DOI: 10.1134/S1063783411060266

1. INTRODUCTION

The possibility of preparing a cubic elpasolite-like structure (space group $Fm\bar{3}m$, $Z = 4$) in many $A_2A'MeO_3F_3$ (A, A': K, Rb, Cs; Me: Mo, W) compounds with mixed ligands forming a six-coordinated MeO_3F_3 polyhedron was established for the first time many years ago [1]. A similar structure can exist at the relationship between ionic radii of univalent cations as follows: $R_A > R_{A'}$. IR spectroscopy has shown that the local symmetry of the octahedron is orthorhombic (C_{3v}), which is due to the fac-configuration of ligands. One of reasons for the high symmetry of the oxyfluoride crystal lattice is assumed to be the absence of correlation in mutual orientations of the MeO_3F_3 groups over the crystal volume. Thus, it is reasonable to suppose that polar states can be formed in $A_2A'MeO_3F_3$ crystals as a result of ordering of the structure due to correlated rotations of the octahedra.

The temperature dependences of some physical properties of $A_2A'MeO_3F_3$ (Me: W, Mo) oxyfluorides were for the first time studied in [2]. Unlike [1], only $Cs_2KMeO_3F_3$ and $Rb_2KWO_3F_3$ have the cubic structure at room temperature (293 K). This contradiction is quite strange, since, in both cases [1, 2], the compounds were prepared by the same very simple technology, namely, by the solid-state reaction $MeO_3 + 2AF + A'F \longrightarrow A_2A'MeO_3F_3$ at ~600°C. Depending on the relationship between ionic radii R_A and $R_{A'}$ and also the type of Me atom, the $Fm\bar{3}m$ structure could remain stable at least to liquid-nitrogen temperatures ($Cs_2KMeO_3F_3$) or be distorted as a result of one ($Cs_2RbMeO_3F_3$ and $Rb_2KWO_3F_3$) and two phase transitions ($Rb_2KMoO_3F_3$). In all cases, the transition from the cubic phase was accompanied by the formation of a spontaneous polarization, and the second phase transition in $Rb_2KMoO_3F_3$ was assumed to be due to the nonferroelectric nature [3].

The structural studies were performed only on a $Rb_2KMoO_3F_3$ single crystal and only in its paraelectric phase, since, in the low-temperature phases, the ferroelastic twinning hampering the structure refinement was revealed [4]. It was found that the F and O atoms that statistically equally probably occupy the same crystallographic positions 24*e* are characterized by a pronounced anisotropy of vibrations and the largest thermal parameter as compared to other atoms. Thus, the ligands or the octahedron as a whole can determine the mechanism of distortion of the structure.

The change in the degree of disordering of the structural elements during a phase transition is quan-

titatively determined by the corresponding change in the entropy that is substantially different for displacive ($\Delta S \ll R\ln 2$) and order–disorder ($\Delta S \geq R\ln 2$) transformations [5]. Unfortunately, there are no relevant data for elpasolites $A_2A'MeO_3F_3$. However, in [3], the data on the enthalpy and entropy of phase transitions are presented for related cryolites $A_3MeO_3F_3$ in which the A and A' atoms in positions 8*c* and 4*b* are identical. Independently of the combination of cations, cryolites undergo two successive transitions that are characterized by the nature identical to that of transformations in $Rb_2KMoO_3F_3$. The entropy changes for different crystals and transitions vary within the limits of $\Delta S = R\ln 1.3 - R\ln 2.2$, and the summary change for two transformations is $\Sigma\Delta S_i = R\ln 1.9 - R\ln 3.9$. These data suggest that the cubic phase of cryolites $A_3MeO_3F_3$ can contain some disordered structural elements. Most likely, they are MeO_3F_3 octahedra ordered during the ferroelectric transition, which favors the appearance of the macroscopic polarization.

The fact that the octahedra can actively participate in the phase transition mechanisms, at least, in the molybdenum elpasolites either themselves or due to implantation of tetrahedral cations into the structure, can be demonstrated by the data on studying elpasolite $(NH_4)_2KMoO_3F_3$ and cryolite $(NH_4)_3MoO_3F_3$ [6, 7]. In both compounds, the entropies of the phase transitions from the cubic phase were close: $R\ln 4.8$ and $R\ln 5$, respectively. These values slightly but do exceed the summary entropies observed in cryolites with atomic cations [3].

Recent studies of the thermodynamic properties of $(NH_4)_3TiOF_5$ [8] and Rb_2KTiOF_5 [9] with the tetragonal symmetry of the octahedra have shown that the cation substitution $Rb_2K \longrightarrow (NH_4)_3$ does not practically influence the entropy change: it is $\Delta S \approx R\ln 8$ in both oxyfluorides. However, in this case, the hydrostatic-pressure susceptibility, which is an indirect characteristic of a structural disorder, increases anomalously (from 6 to 110 K/GPa).

The oxyfluorides with a combination of atomic cations K_2Na have not been practically studied. Only it was known that $K_2NaMeO_xF_{6-x}$ (*Me*: W^{6+}, Mo^{6+}, V^{5+}, V^{4+}, and Ti^{4+}) crystals have the cubic elpasolite structure at room temperature [1].

In the light of the foregoing, the study of the thermodynamic properties of elpasolites $A_2A'MeO_3F_3$ is of undeniable interest. In this work, we studied (1) the heat capacity, the susceptibility to external pressures, the permittivity, and the structure of the cubic phase of the $Rb_2KMoO_3F_3$ crystal and (2) temperature limits of stability of the $Fm\bar{3}m$ cubic phase in elpasolite $K_2NaMoO_3F_3$.

Table 1. Unit cell parameters a_0, temperatures T_1, and enthalpies ΔH_1 of the transition from the $Fm\bar{3}m$ phase in $Rb_2KMoO_3F_3$ samples synthesized by various methods

Sample no.	a_0, Å	T_1, K	ΔH_1, J/mol	References
1	8.917			[5]
2	8.945*	328		[6]
3	8.929	193	2200	This work
4	8.913	210	1800	The same
5	8.912	187	1000	"
7	8.941	191	2000	"

* The data were obtained at 330 K.

2. SYNTHESIS AND CHARACTERIZATION OF THE SAMPLES. SEARCHING STUDIES

The $Rb_2KMoO_3F_3$ compound was synthesized many times by several methods. In what follows, for the sake of convenience of comparing the sample parameters with available literature data and between them, we will use the numbering as follows: no. 1—[1], no. 2—[2], and so on according to the text.

At the first stage, $Rb_2KMoO_3F_3$ was synthesized from the melt following the method similar to that used earlier [4]. The stoichiometric mixture of MoO_3, RbF, and KF compounds was heated in an oxygen atmosphere in a vertical gradient furnace for three stages, and it was held at 800°C for 10 min and at 950°C for 20 h. After heating to 1050°C, the ampoule with the sample was dropped from the hot zone at a rate of 1.75 mm/h at a temperature gradient of ~15°C/cm. As a result, the polycrystalline $Rb_2KMoO_3F_3$ sample (no. 3) with inclusions of small single-crystal regions was obtained. The study of the compound synthesized using a D8-ADVANCE powder X-ray diffractometer showed that the symmetry at room temperature is cubic ($Fm\bar{3}m$). It agrees with the data of [1] and contradicts to [2], where a pseudotetragonal distortion of the crystal lattice was revealed. The cubic unit cell parameters are given in Table 1.

The quest of phase transitions using a DSM-10M differential scanning microcalorimeter (DSM) allowed us to reveal only one anomaly of the heat capacity near 190 K instead of two transitions found earlier in [2] at 328 ± 5 and 182 ± 5 K. The structural origin of the transformations in sample no. 3 follows from the appearance of splitting of the structural reflections in the X-ray diffraction patterns measured at 120 K. The results of observations using a polarizing microscope agree with the X-ray diffraction and calorimetric data: sample no. 3 isotropic at room temperature becomes anisotropic at ~190 K.

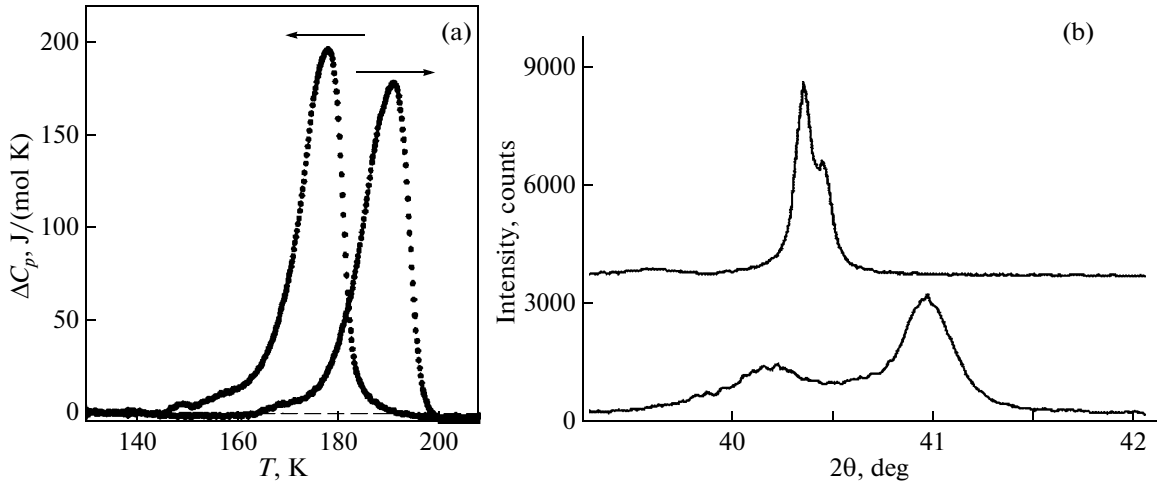

Fig. 1. (a) Excess heat capacity of $Rb_2KMoO_3F_3$ vs. temperature according to the DSM measurement during heating and cooling and (b) (400) reflection in the high-temperature and low-temperature phases.

Sample no. 4 was prepared from the same initial components by the solid-phase synthesis used earlier in [1, 3]. A mixture of carefully dried reagents was three times held in vacuum at a temperature of 600°C for 48 h with intermediate grinding the mixture. The required oxyfluoride $Rb_2KMoO_3F_3$ also undergoes one transition but at higher temperature and with smaller value of ΔH_1 as compared to sample no. 3 (Table 1). It seems quite probable that the increase in T_1 and decrease in ΔH_1 and also a_0 were due to the existence of foreign phases revealed by the X-ray diffraction studies in the sample.

Further, $Rb_2KMoO_3F_3$ was also synthesized by several versions of reactions, a part of which is given below:

Sample no. 5: $(NH_4)_3MoO_3F_3 + Rb_2CO_3 + 0.5K_2CO_3 = Rb_2KMoO_3F_3 + 3NH_3\uparrow + 1.5CO_2\uparrow + 1.5H_2O\uparrow$.

Sample no. 6: $MoO_3 + NH_4HF_2 + Rb_2CO_3 + KF = Rb_2KMoO_3F_3 + NH_3\uparrow + CO_2\uparrow + H_2O\uparrow$.

In both cases, the mixture was heated for three stages: (1) at 200–300°C with mixing for fast removal of water; (2) in a muffle furnace at 600°C; and (3) at 750–800°C for 30–40 min.

Single-crystal sample no. 7 several mm^3 in volume was prepared, as samples nos. 3 and 4, from KF, RbF, and MoO_3. However, in the latter case, we used specific methods of preparing anhydrous initial reagents. The synthesized $Rb_2KMoO_3F_3$ powder was placed in a platinum crucible, at whose bottom, fluoroplastic chips as a fluorine agent were sent, and it was heated to 900°C at a rate of 100°C/h. The furnace was turned off immediately after heating. The rate of the initial decreasing temperature was about 100°C/h.

We used eight various methods of preparing $Rb_2KMoO_3F_3$. All the samples were cubic at room temperature and none of them had the parameters characteristic of the sample studied in [3]. It should be noted that the anomaly of the heat capacity and appearance of the optical anisotropy in our synthesized samples are observed at a temperature very close to the temperature of the low-temperature ferroelectric transition (185 ± 5 K) that was observed in [3]. Thus, we did not reveal a ferroelectric phase transition. It is likely very useful to study oxyfluoride we prepared, since its state is most easy realized and stable.

Based on preliminary X-ray diffraction, calorimetric, and optical data, sample no. 7 has the most optimal quality parameters (absence of impurities, a small width of X-ray diffraction reflections, a shape of the anomaly of the heat capacity, transition enthalpy, and optical transparency). Because of this, sample no. 7 was studied in more detail. An analysis performed on an X-ray fluorescence spectrometer shows that the relationship between the real and calculated contents of individual elements in the $Rb_2KMoO_3F_3$ sample is quite satisfactory (the differences do not exceed 0.3–0.5%).

Figure 1a shows the temperature dependence of the heat capacity of $Rb_2KMoO_3F_3$ (sample no. 7) found from the DSM data measured during heating and cooling the sample in the temperature range 110–350 K.

The temperature of the heat capacity maximum in the heating regime and the phase transition enthalpy are given in Table 1. Thermal hysteresis during the phase transition found by thermal cycling is $\delta T_0 = 13$ K.

Below the transition temperature from the cubic phase, the powder X-ray diffraction of $Rb_2KMoO_3F_3$ clearly demonstrates the splitting of the structure reflection (400) (Fig. 1b), as is the case with

$(NH_4)_2KMoO_3F_3$ [6]. This fact can testify that the structure distortions in molybdenum elpasolites are close, unlike cryolite $(NH_4)_3MoO_3F_3$, where no splitting was observed [7].

Oxofluorinomolybdate $K_2NaMoO_3F_3$ was synthesized by two methods: MoO_3 and $(NH_4)_2MoO_3F_3$ were used, respectively. The initial components were mixed in stoichiometric proportions according to reactions

$$MoO_3 + 2KF + NaF = K_2NaMoO_3F_3,$$

$$(NH_4)_2MoO_3F_2 + NaF + 2KOH = K_2NaMoO_3F_3 + 2NH_3 + 2H_2O.$$

The synthesis was carried out in the sequence that was used during preparing $Rb_2KMoO_3F_3$ samples (nos. 5 and 6).

The studies on the powder X-ray diffractometer show that, at room temperature, $K_2NaMoO_3F_3$ synthesized has the cubic lattice (space group $Fm\bar{3}m$) with the parameter $a_0 = 8.398$ Å that satisfactorily corresponds to $a_0 = 8.393$ Å reported in [1]. The experiments performed at 100 K did not reveal any marked changes in the X-ray diffraction pattern as compared to similar that measured at high temperatures. The calorimetric studies of $K_2NaMoO_3F_3$ by the DSM method in the range 110–300 K do not reveal anomalies of the heat capacity. A set of the obtained experimental data can be interpreted assuming that $K_2NaMoO_3F_3$ does not undergo any structural phase transitions, at least, in the temperature range under study.

Thus, the stability of the elpasolite phase of $A_2A'MeO_3F_3$ crystals is retained in a wide temperature range not only for the Cs_2K cation combination [2] but also for K_2Na, as it follows from our data.

3. HEAT CAPACITY, HYDROSTATIC PRESSURE SUSCEPTIBILITY, AND PERMITTIVITY OF $Rb_2KMoO_3F_3$

The thermodynamic parameters of the phase transition in $Rb_2KMoO_3F_3$ were refined using an adiabatic calorimeter. The heat capacity was measured on the 1.93-g sample in the temperature range 85–330 K using the regimes of discrete ($\Delta T = 1.8$–2.5 K) and continuous ($dT/dt = 0.18$–0.22 K/min) heatings. A copper container filled with the powder sample was hermetically packed into an indium capsule that, in turn, was enveloped with an aluminum polished foil with a glued on a constantan-wire heater. The heat capacity of the furniture (foil, heater, copper and indium capsules) was measured in a specific experiment. Hysteresis phenomena in the vicinity of the phase transition were studied using a method of quasi-static thermograms on heating and on cooling ($|dT/dt| \approx 0.02$ K/min).

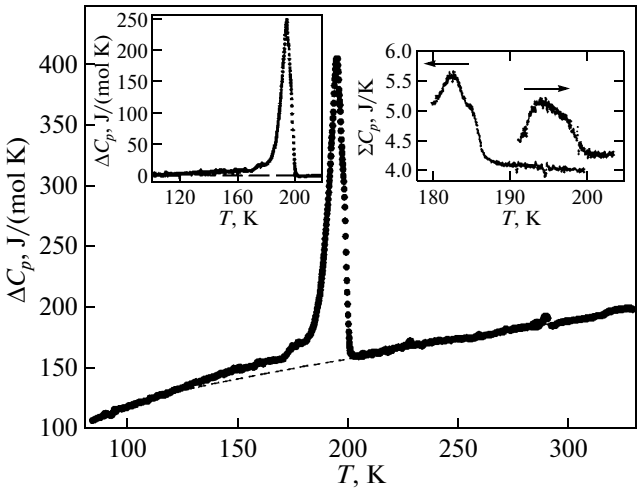

Fig. 2. Temperature dependence of the molar heat capacity of $Rb_2KMoO_3F_3$. The dashed line shows the lattice heat capacity. The inset shows (at the right) the heat capacity of the "sample + furniture" system near the phase transition measured by the method of thermograms during heating and cooling and (at the left) the excess heat capacity of $Rb_2KMoO_3F_3$.

The measured temperature dependence of the heat capacity of $Rb_2KMoO_3F_3$ is shown in Fig. 2. It is seen that, as well as in the DSM experiment, the pronounced anomalous behavior of the heat capacity is only observed near 190 K. Above a room temperature, where, according to [2], as though $Rb_2KMoO_3F_3$ undergoes a ferroelectric transition, the anomaly of the heat capacity was not revealed. The refined structural transition temperature and its hysteresis were $T_1 = 194.6 \pm 0.1$ K and $\delta T_1 = 12$ K, respectively. It would be noted that the hysteresis width is slightly changed as compared to the DSM data despite the substantial decrease in the temperature scanning rate in the experiments with the adiabatic calorimeter. This fact testifies that the transition under study is significantly far from the tricritical point. We did not observe a pronounced enthalpy jump during the transition, which can be due to spreading the heat capacity anomaly in the powder sample (right inset to Fig. 2).

Figure 2 shows also a small heat capacity anomaly near $T_2 \approx 175$ K that is clearly manifested in the temperature dependence of the excess heat capacity (left inset to Fig. 2). To select the latter from the heat capacity measured, its lattice component was found by both a polynomial approximation of the experimental data far from the phase transition and also using the Debye and Einstein equations. The results obtained by the two methods differ insignificantly. As a criterion of comparing the two variants of approximation, we used the enthalpy change during the phase transition determined by integration of the $\Delta C_p(T)$ function over entire temperature range of existence of the anoma-

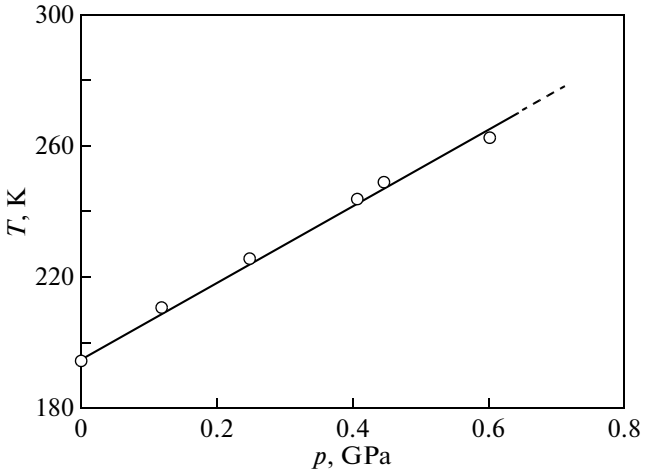

Fig. 3. T–p phase diagram of $Rb_2KMoO_3F_3$.

lous heat capacity. In the first case, the ΔH_1 enthalpy was 2500 J/mol, and, in the second case, 2770 J/mol.

Thus, the difference does not exceed 10%, and as the final value, the average value $\Delta H_1 = 2640 \pm 150$ J/mol was taken.

The corresponding entropy change during the phase transition in $Rb_2KMoO_3F_3$ is $\Delta S_1 = \int(\Delta C_p/T)dT = 14.3 \pm 0.8$ J/(mol K).

The maxima of the heat capacity anomalies at T_1 and T_2 are different by a factor of almost 25 (left inset to Fig. 2); because of this, there is no point in separating the related integral parameters, since the thermal effect at T_2 will undoubtedly be comparable with the error of determination of the effect at T_1.

Despite the existence of the anomalous heat capacity in a wide temperature region of the distorted phase, its behavior does not described in terms of the Landau phenomenological theory [10], i.e. the $(\Delta C_p(T)/T_0)^{-2}$ is not linear even near the phase transition temperature. This is particularly true for an analysis of the excess heat capacities determined by two methods described above. This fact undoubtedly underlines once again a significant distance in temperature of the transition in $Rb_2KMoO_3F_3$ from the tricritical point.

The susceptibility of $Rb_2KMoO_3F_3$ to high hydrostatic pressures was studied by the DTA method on the device described in [11] that we repeatedly used to study the temperature–pressure phase diagrams of many oxyfluorides and fluorides [5–9]. The powder sample was placed into a copper container ~0.03 cm^3 in volume attached to one of junction of a sensitive copper–germanium thermocouple element inserted in a cylinder–piston-type high-pressure chamber connected to a multiplier.

Figure 3 shows the results of the study as the temperature–pressure phase diagram. The phase boundary is a straight line described by the equation $T_1(p) = 195 + 117p$ in the pressure range under study (to 0.06 GPa). The anomaly at T_2 was not revealed in the experiments under pressure.

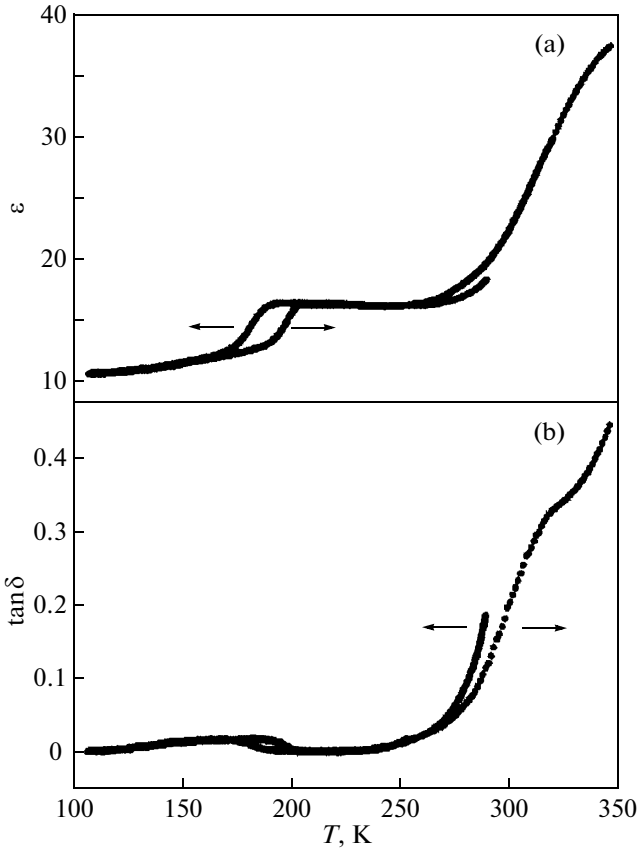

Fig. 4. (a) Dielectric permittivity and (b) loss tangent during heating and cooling of the oxyfluoride $Rb_2KMoO_3F_3$ versus temperature.

The permittivity was measured using an E7-20 immittance meter at a frequency of 1 kHz on heating and on cooling at a rate of ~0.6 K/min in the temperature range 100–350 K including the temperature of the ferroelectric phase transition assumed in [3]. Since we failed to grow the single crystals of a fairly large volume, the studies were carried out on a ceramic sample in the form of a pellet 8 mm in diameter and 2 mm in height prepared of a fine-disperse powder by its pressing and heat treatment. The copper electrodes were deposited in vacuum.

Figure 4 depicts the results of measurements of $\varepsilon(T)$ and $\tan\delta(T)$. The permittivity is slowly changed from 10 to 13 units in a wide temperature range as the transition is approached (Fig. 4a). Near the transition at T_1, ε increases quickly to 16–17 units, and then it remains practically constant to 250 K, where it quickly increases again to 37 units. It should be noted that the dielectric losses behave similarly increasing by a factor of approximately 200 (Fig. 4b). The fairly quick

Table 2. Crystallographic and experimental data of the X-ray diffraction studies of $Rb_2KMoO_3F_3$

T, K	Radiation	Total number of reflections	Number of independent reflections	Reflections with $F_{hkl} \geq 4\sigma_F$	R_{int}/R_σ	Space group	Number of formula units Z	a, Å
298	MoK_α	1929	74	63	0.0358/0.0133	$Fm\bar{3}m$	4	8.941(8)

Table 3. Coordinates of atoms in $Rb_2KMoO_3F_3$, position occupancy (q), and thermal parameters (U)

Atom	X	Y	Z	q	U, Å^2
Mo	0	0	0	1	$U_{11} = U_{22} = U_{33} = 0.0324(6)$
Rb	1/4	1/4	1/4	1	$U_{11} = U_{22} = U_{33} = 0.0327(6)$
K	1/2	0	0	1	$U_{11} = U_{22} = U_{33} = 0.0168(7)$
F	0.2118(6)	0	0	0.5	$U_{11} = 0.018(3)$; $U_{22} = U_{33} = 0.060(3)$
O	0.2118(6)	0	0	0.5	$U_{11} = 0.018(3)$; $U_{22} = U_{33} = 0.060(3)$

change in ε in the vicinity of the phase transition at T_1 can be quite considered as a jump spread in the ceramic sample. According to [12], such a behavior of the permittivity is characteristic of first-order nonferroelectric phase transitions. The hysteresis $\delta T_1 = 15$ K (Fig. 4a) observed in these measurements is close to the values found in the experiments with DSM and adiabatic calorimeter.

4. CRYSTAL STRUCTURE

The X-ray diffraction experiment on $Rb_2KMoO_3F_3$ was performed using a SMART APEXII single-crystal diffractometer with an x–y detector and with monochromatized MoK_α radiation (λ = 0.7106 Å). The studies were carried out at room temperature and at 100 K. It should be noted that the low-temperature experiment was not quite successful. The change in the crystal lattice symmetry at $T < T_1$ is evident according to the reflection splitting (Fig. 1). However, most likely, due to the ferroelastic nature of the transition at T_1, a too complex twin structure appears so, that the twinning law for the purpose of refining the crystal structure cannot be chosen.

The orientation matrix and the unit cell parameters at room temperature are determined and refined from 152 reflections. The unit cell corresponds to the cubic system. Main crystallographic characteristics and the parameters of the experiment are given in Table 2.

The quest of the structural model was performed by direct methods using the SHELXS program [13]. As a result, the coordinates of all the atoms were found. The structure obtained was refined by the least square method using the SHELXL97 program [14]. The thermal parameters of all the atoms were refined in an anisotropic approximation. As a result, we found the final structure model, the refinement of which was completed at $R = 0.0183$ for 63 reflections with $|F_{hkl}| > 4\sigma_F$, $R1 = 0.0237$ and $wR2 = 0.0489$ for all 74 independent reflections and the fitting quality GooF = 1.039. The results of the structure refinement are presented in Table 3.

5. ANALYSIS OF THE RESULTS

In this work, we have studied numerous $Rb_2KMoO_3F_3$ samples prepared by various methods and have not found a ferroelectric phase transition that, according to [3], as if exists at 328 K. At the present time, we cannot explain the observed discrepancy of the data. At the same time, it should be noted that there is a satisfactory agreement between the temperatures of the ferroelastic transformation near 180–190 K found in this work and in [3]. Against this background, it is of a high interest to compare the thermodynamic parameters of nonferroelectric phase transitions in a number of fluorine–oxygen elpasolites $Rb_2KMeO_xF_{6-x}$ ($x = 0, 1, 3$) [15–17] having the same cation combination and different in the composition of ligands and, correspondingly, the valence of the central atom (Table 4). The transition temperature hysteresis, the entropy, and the susceptibility to hydrostatic pressure are very close, and they are slightly dependent on the composition of the six-coordinated polyhedron. It should be noted as well that the rela-

Table 4. Thermodynamic parameters of the transition from the $Fm\bar{3}m$ phase in elpasolites $Rb_2KMeO_xF_{6-x}$ ($x = 0, 1, 3$)

Crystal	T_1, K	δT_1, K	ΔS_1, J/(mol K)	dT_1/dp, K/GPa
$Rb_2KMoO_3F_3$	195	12	14.3	117
Rb_2KTiOF_5 [15]	215	6	17	110
Rb_2KFeF_5 [16]	180	4.6	15.6	132
Rb_2KGaF_6 [17]	123	6	14.4	112

tionship between the thermal parameters of atoms in these elpasolites is approximately the same, and the least parameter is characteristic of the atom in the position 4*b* (Table 3, [15]). A set of these data is thought can testify that the octahedron subsystem does not play a determining role in the mechanism of the transition from the cubic phase.

It is appropriate to analyze the data, considering, in particular, a number of compounds containing the MoO_3F_3 octahedron in the elpasolite-like structure and different in the cation composition: Rb_2K (T_1 = 194 K) ⟶ $(NH_4)_2K$ (T_1 = 240 K) [6] ⟶ $(NH_4)_3$ (T_1 = 297 K) [7] ⟶ K_2Na. All the crystals, exception for $K_2NaMoO_3F_3$ that is stable at least to 100 K, according to our measurements, undergo first-order phase transitions apart in temperature from the tricritical point. The transition temperatures decrease as spherical cations are substituted for the ammonium tetrahedral cation. This experimental fact satisfactorily agrees to the regularity in the relationship between the temperatures T_1 for the cubic oxyfluorides with univalent atomic cations in both crystallographic positions (4*b* and 8*c*) [3]: cryolites undergo the transition at higher temperatures comparing to elpasolites. The phase transitions in molybdates have different nature. The distorted phase of cryolite $(NH_4)_3MoO_3F_3$ [7] is ferroelectric, and those of elpasolites $(NH_4)_2KMoO_3F_3$ [6] and $Rb_2KMoO_3F_3$ are ferroelastic.

It is of interest to consider the data for a number of molybdenum elpasolites-cryolites, among them the data obtained in [3], regarding the cubic phase unit cell parameters and temperatures of its stability in terms of hypothesis on the strengths of interatomic bonds. The essence of this approach is that the stability of the initial cubic structure of perovskite-like crystals is determined by the relationship between ionic radii of individual atoms and the lattice parameters a_0 [18]. Early, such an analysis was performed for the transitions from the $Fm\bar{3}m$ phase in the related fluorides with the elpasolite structures $Rb_2KB^{3+}F_6$ (B^{3+}: Ga, Cr, Fe, Sc, In, Lu, Dy) and cryolite structures $(NH_4)_3B^{3+}F_6$ (B^{3+}: Ga, Al, Cr, Fe, V, Sc, In) by estimating the ion bond strength in the chains $A^+(8c)$–F^- (24*e*)–μ_A and $B^{3+}(4a)$–F^-–$A'(4b)$–F^-–B^{3+}–μ_B [5, 19]. The hypothesis is fruitful for both the displacive transitions and the transformations related to processes of ordering. It was elucidated that the symmetry of the phase formed during the transition does not play any role. At the same time, it was established that one of conditions of applicability of the hypothesis is an imperative relation of the transitions with rotations of the octahedral ionic groups. In other case, such as for two series of fluorine cryolites $Rb_2B^{3+}F_6$ and $Cs_3B^{3+}F_6$ (B^{3+}: Ga, In, Dy) that undergo the transitions accompanied by atomic displacement leading, in particular, to significant distortions of the octahedra, the hypothesis is inadequate [5, 20]. As a quantitative measure of the interatomic bond strengths, the quantities were proposed in [19] that, for compounds with fluorine–oxygen ligands $A_2A'MO_3F_3$, have the form as follows [5]: $\mu_A = (a_p' - a_0)/a_p'$, $\mu_B = (a_p - a_0)/a_p$, where $a_p = 2(R_{A'} + 2R_{F/O} + R_M)$ and $a_p' = 2\sqrt{2}(R_A + R_{F/O})$. Here, $R_{F/O}$ is the mean ion radius determined as $(R_O + R_F)/2$. An increase in μ_B is equivalent to an increase in the repulsion energy in the crystal potential, and it leads to "pressing-out" of the F/O atoms from the position 24*e* at the unit cell edge, i.e., to an increase in the anisotropy and/or anharmonicity of their motion and, thus, to a decrease in the stability of the initial cubic phase, namely, to an increase in the transition temperature. On the other hand, the increase in μ_A hinders the displacement of ligands from the position 24*e* and favor the stabilization of the undistorted cubic lattice.

In some molybdenum oxyfluorides, the entropies of transition from the cubic phase are very close and large, which is characteristic of the order–disorder processes: $R\ln 4.8$ in $(NH_4)_2KMoO_3F_3$ [6], $R\ln 5$ in $(NH_4)_3MoO_3F_3$ [7], and $R\ln 5.6$ in $Rb_2KMoO_3F_3$. Thus, despite that there are no data on the structure of the low-temperature phases of these crystals, we cannot exclude a possibility of certain relation of the transformation mechanism with a rotation of the six-coordinated $[MoO_3F_3]$ polyhedra.

Figure 5 shows the $\mu_A(a_0)$ and $\mu_B(a_0)$ dependences for molybdates with the cation composition $(NH_4)_2NH_4$ ⟶ $(NH_4)_2K$ ⟶ Rb_2K ⟶ Cs_2K ⟶ K_2K ⟶ K_2Na studied in this work and in [3]. In $K_3MoO_3F_3$, the transition from the $Fm\bar{3}m$ phase takes place at 522 K [3], while, in other oxyfluorides under consideration, the transitions occurs at substantially lower temperatures. Because of this, a comparison of the bond strengths of different crystals can be correct only as the unit cell parameters found at the same temperature are used.

We measured the thermal expansion coefficients of oxyfluorides $A_2A'MoO_3F_3$ (*A*, *A*': K, Rb, NH_4) using a NETZSCH DIL-402C inductive dilatometer. Beyond the phase transition region for different crystals, the coefficient are varied within the limits $(1.5–3.0) \times 10^{-5}$ K^{-1}.

The correction to the value a_0 by extrapolating to a temperature of 550 K at which the unit cell parameter in $K_3MoO_3F_3$ was found to be ~1%. It is seen from Fig. 5 that both bond strengths increase as the unit cell parameter decreases for the combinations $(NH_4)_2NH_4$ ⟶ $(NH_4)_2K$ ⟶ Rb_2K ⟶ K_2K. The exceptions are the compounds with K_2Na and Cs_2K cations for which μ_A and μ_B are the maximal and minimal, respectively, despite the large difference in a_0. These oxyfluorides

are precisely those that do not undergo phase transition at least to ~100 K [2, 3]. An increase in the temperature of the cubic phase stability loss in a number of molybdates with the cation combinations Rb_2K, $(NH_4)_2K$, and $(NH_4)_2NH_4$ (Fig. 5) is, at first glance, strange, since it is result of an increase in both μ_A and μ_B. However, the bond strength μ_A that hinders the rotation of the octahedral (displacement of ligands to interoctahedral void) decreases significantly faster. Only cryolite $K_3MoO_3F_3$ does not fit in the total tendency, since it has maximal values of μ_A and μ_B and also the maximum transition temperature (Fig. 5). It remains to assume, based on the results of an analyses performed in [5, 20], that the transition in $K_3MoO_3F_3$ is not accompanied by rotations of the octahedra. This assumption is confirmed by relatively small entropy change $\Delta S < R\ln 2$ [3].

According to model concepts of a disorder in the elpasolite–cryolite cubic structure based on structural studies [5, 21, 22], the transition entropy can be due to the processes of orientation ordering of the MO_3F_3 octahedra and NH_4 tetrahedra (in the position 4*b*) and also position ordering of spherical cations in the position 8*c*.

The ligand vibration anisotropy in $Rb_2KMoO_3F_3$ (Table 3) is very significant, and it even exceeds the anisotropy in ammonium-containing oxyfluorides $(NH_4)_2KMoO_3F_3$ ($U_{11} = 0.016$ Å^2, $U_{22} = U_{33} = 0.030$ Å^2) [6], and $(NH_4)_3MoO_3F_3$ ($U_{11} = 0.026$ Å^2, $U_{22} = U_{33} = 0.045$ Å^2) [7].

The X-ray diffraction patterns of the distorted phases of the molybdenum elpasolite and cryolite are different: in $(NH_4)_3MoO_3F_3$ [7], there is no splitting of the structure reflections characteristic of $(NH_4)_2KMoO_3F_3$ [6] and $Rb_2KMoO_3F_3$. On the other hand, under pressure, the stability of the cubic phase decreases ($dT_1/dp > 0$) in $(NH_4)_3MoO_3F_3$ [7] and $Rb_2KMoO_3F_3$ and increases ($dT_1/dp < 0$) in $(NH_4)_2KMoO_3F_3$ [6]. Both experimental facts undoubtedly demonstrate significant individual features of details of the mechanisms of structural distortions in these oxyfluorides. It seems quite possible that, in the ammonium-containing crystals, the noted facts are due to various proportions of tetrahedral cations in the structure. In the cryolite, the ammonium cation in the position 4*b* is necessarily disordered, and, in this case, disordering of the tetrahedron in the position 8*c* is most likely hampered. In the elpasolite structure, the ammonium cation in the position 8*c* also can contribute to the mechanism of structural distortions. Its tops lie at the third-order axes and, thus, the N–H...F(O) bond can be disordered in three directions.

One of possible reasons of a fairly large transition entropy in $Rb_2KMoO_3F_3$, along with rotation of the octahedral, can be, e.g., a disordering or pronounced anharmonicity of vibrations of the atomic cations in

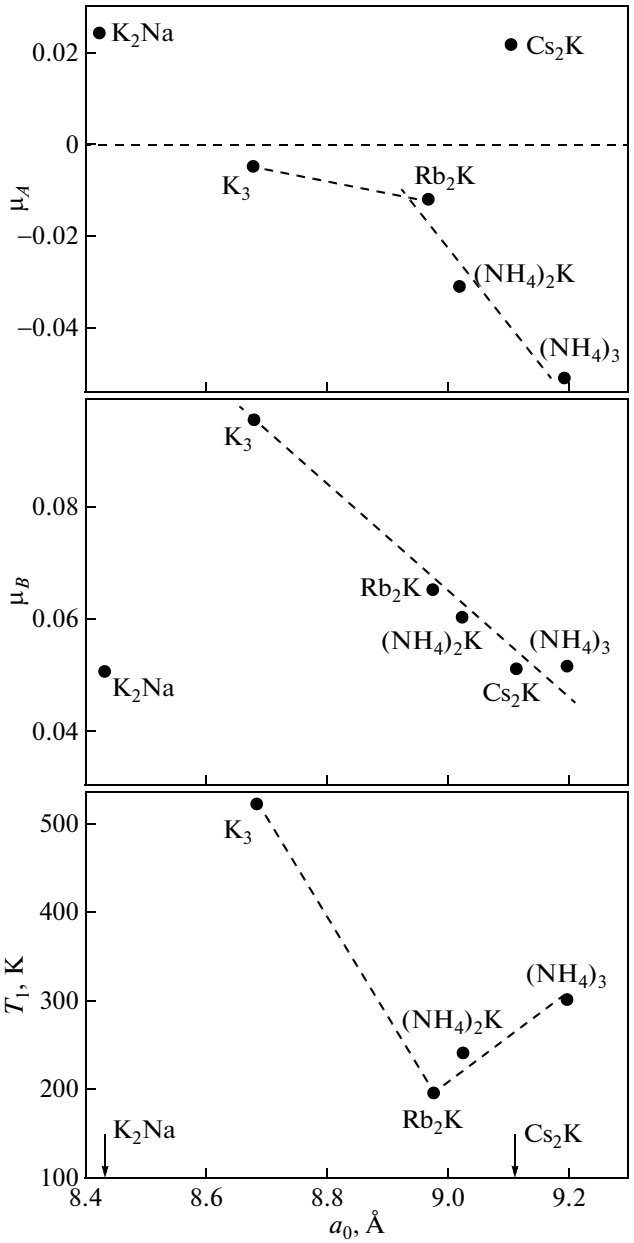

Fig. 5. Dependences of μ_A, μ_B, and phase transition temperatures of $A_2A'MoO_3F_3$ crystals on the cubic unit cell parameters.

the $Fm\bar{3}m$ phase. The thermal parameters of the Mo, Rb, and K atoms are quite different (Table 3). It seems quite probable that the contribution of the ordering and displacement of the Mo and Rb atoms to the transition entropy can be very large.

Above, we told about a relationship of the transitions from the cubic phase in fluorine and fluorine–oxygen crystals with the general formula $Rb_2KMeO_xF_{6-x}$ ($x = 0, 3, 5$). Their common properties are, in particular, large values of the entropy and the pressure coefficient. Materials characterizing by

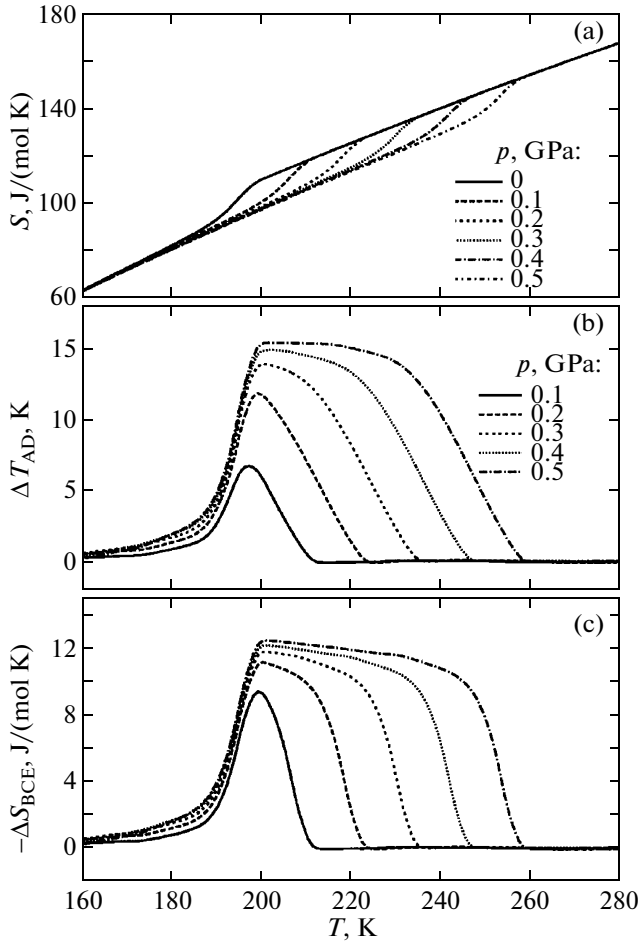

Fig. 6. (a) Temperature dependences of the change in the total entropy of $Rb_2KMoO_3F_3$ in the range 160–280 K and (b) intensive and (c) extensive barocaloric effects.

such parameters can have a significant barocaloric effect (BCE). The essence of the effect is a reversible change in the entropy ΔS_{BCE} (temperature ΔT_{AD}) of a thermodynamic system as external pressure is varied in isothermal (adiabatic) conditions.

Recently, an analysis of the barocaloric effect was performed for Rb_2KTiOF_5 [23]. The maximum values of the extensive $\Delta S_{BCE} = -46$ J/(kg K) and intensive $\Delta T_{AD} = 18$ K barocaloric effect realized at a pressure of ~0.5 GPa are comparable with the parameters of the magneto- and electrocaloric effects in materials considered as promising solid-state coolants [24, 25]. To estimate ΔS_{BCE} and ΔT_{AD} in $Rb_2KMoO_3F_3$, we used the same approach that was used in [23]. The change in the total entropy of the crystal with temperature and pressure was determined by summing the lattice component $S_L(T) = \int(C_p/TdT)$ (independent of pressure) and the anomalous entropy $\Delta S(T) = \int(\Delta C_p/T)dT$ related to the transition (Fig. 6a). Since the studies of the $T_1(p)$ dependence stated that the transition entropy remains unchanged in the pressure range under study, the transition temperature (the inflection point in $\Delta S(T)$ in Fig. 6a), with allowance for the pressure coefficient, was shifted with the pressure as $S(T, p) = S_L(T) + \Delta S(T + pdT/dp)$. The extensive BCE magnitude was determined as the difference of the total entropies under pressure and without pressure $\Delta S_{BCE}(T, p) = S(T, p \neq 0) - S(T, p = 0)$ at a certain constant temperature. The intensive BCE was calculated using the relationship $\Delta T_{AD} = -(T/C_p)\Delta S_{BCE}$.

Figures 6b and 6c depict the pressure and temperature dependences of the extensive and intensive BCE for $Rb_2KMoO_3F_3$. The maximum magnitudes of the effects $\Delta T_{AD}^{max} \approx 16$ K and $\Delta S_{BCE}^{max} \approx -12.5$ J/(mol K) = -30 J/(kg K) are somewhat smaller than the limiting parameters of Rb_2KTiOF_5 [23] at the approximately same pressure ~0.5 GPa.

6. CONCLUSIONS

We have synthesized the $K_2NaMoO_3F_3$ and $Rb_2KMoO_3F_3$ compounds. The cubic structure of the former oxyfluoride is stable at least to 100 K, according to the data of calorimetric and X-ray diffraction studies. In numerous samples of the latter crystal prepared by various methods, we did not reveal a ferroelectric phase transition near 328 K as reported in [3]. At the same time, the temperature of nonferroelectric structural transformation in our samples (194.5 K) is close to that (182 ± 5 K) found in [2, 3].

We studied in detail the thermodynamic and dielectric properties and the cubic phase structure in $Rb_2KMoO_3F_3$. It was established that the phase transition in this oxyfluoride is a first-order order–disorder-type transformation distant from the tricritical point. An analysis of the barocaloric efficiency showed that the magnitudes of the extensive and intensive effects for $Rb_2KMoO_3F_3$ are comparable with the parameters of solid-state coolants.

It was shown that oxyfluorides $Rb_2KMeO_xF_{6-x}$ ($x = 0, 1, 3$) are characterized by similarity of the thermodynamic parameters: significant values of the thermal hysteresis, transition entropy, and pressure coefficient.

It was established that the hypothesis on the interatomic bond strengths is applicable for analyzing the limits of the cubic phase stability in the molybdenum-containing elpasolites–cryolites $A_2A'MoO_3F_3$ (A, A': Na, K, Rb, Cs, and NH_4).

ACKNOWLEDGMENTS

We are grateful to S.V. Mel'nikova for presenting the results of polarization optical observations and to

G.V. Bondarenko from analyzing the composition of the oxyfluoride $Rb_2KMoO_3F_3$.

This study was supported by the Siberian Branch of the Russian Academy of Sciences within the framework of the Interdisciplinary Integration project no. 34 SO RAN and the Council on Grants from the President of the Russian Federation for Support of Leading Scientific Schools of the Russian Federation (project no. NSh-4645-2010.2).

REFERENCES

1. G. Pausewang and W. Rüdorff, Z. Anorg. Allgem. Chem. **364** (1–2), 69 (1969).
2. G. Peraudeau, J. Ravez, and H. Arend, Solid State Commun. **27**, 515 (1978).
3. J. Ravez, G. Peraudeau, H. Arend, S. C. Abrahams, and P. Hagenmüller, Ferroelectrics **26**, 767 (1980).
4. S. C. Abrahams, J. L. Bernstein, and J. Ravez, Acta Crystallogr., Sect. B: Struct. Crystaloogr. Cryst. Chem. **37**, 1332 (1981).
5. I. N. Flerov, M. V. Gorev, K. S. Aleksandrov, A. Tressaud, J. Grannec, and M. Couzi, Mater. Sci. Eng., R **24**, 81 (1998).
6. I. N. Flerov, M. V. Gorev, V. D. Fokina, A. F. Bovina, M. S. Molokeev, E. I. Pogorel'tsev, and N. M. Laptash, Fiz. Tverd. Tela (St. Petersburg) **49** (1), 136 (2007) [Phys. Solid State **49** (1), 141 (2007)].
7. I. N. Flerov, V. D. Fokina, A. F. Bovina, E. V. Bogdanov, M. S. Molokeev, A. G. Kocharova, E. I. Pogorel'tsev, and N. M. Laptash, Fiz. Tverd. Tela (St. Petersburg) **50** (3), 515 (2008) [Phys. Solid State **50** (3), 515 (2008)].
8. I. N. Flerov, M. V. Gorev, V. D. Fokina, A. F. Bovina, and N. M. Laptash, Fiz. Tverd. Tela (St. Petersburg) **46** (5), 888 (2004) [Phys. Solid State **46** (5), 915 (2004)].
9. V. D. Fokina, I. N. Flerov, M. S. Molokeev, E. I. Pogorel'tsev, E. V. Bogdanov, A. S. Krylov, A. F. Bovina, V. N. Voronov, and N. M. Laptash, Fiz. Tverd. Tela (St. Petersburg) **50** (11), 2084 (2008) [Phys. Solid State **50** (11), 2175 (2008)].
10. K. S. Aleksandrov and I. N. Flerov, Fiz. Tverd. Tela (Leningrad) **21** (2), 327 (1979) [Sov. Phys. Solid State **21** (2), 195 (1979)].
11. M. V. Gorev, I. N. Flerov, A. Tressaud, D. Denu, A. I. Zaitsev, and V. D. Fokina, Fiz. Tverd. Tela (St. Petersburg) **44** (10), 1864 (2002) [Phys. Solid State **44** (10), 1954 (2002)].
12. B. A. Strukov and A. P. Levanyuk, *Ferroelectric Phenomena in Crystals: Physical Foundations* (Nauka, Moscow, 1983; Springer, Berlin, 1998).
13. G. M. Sheldrick, Acta Crystallogr., Sect. A: Found. Crystallogr. **46**, 467 (1990).
14. G. M. Sheldrick, *SHELXL-97: A Computer Program for Refinement of Crystal Structures* (University of Göttingen, Göttingen, Germany).
15. V. D. Fokina, I. N. Flerov, M. S. Molokeev, E. I. Pogorel'tsev, E. V. Bogdanov, A. S. Krylov, A. F. Bovina, V. N. Voronov, and N. M. Laptash, Fiz. Tverd. Tela (St. Petersburg) **50** (11), 2084 (2008) [Phys. Solid State **50** (11), 2175 (2008)].
16. M. V. Gorev, I. N. Flerov, V. N. Voronov, A. Tressaud, J. Grannec, and J.-P. Chaminade, Fiz. Tverd. Tela (St. Petersburg) **36** (4), 1121 (1994) [Phys. Solid State **36** (4), 609 (1994)].
17. M. V. Gorev, I. N. Flerov, A. Tressaud, and J. Grannec, Fiz. Tverd. Tela (St. Petersburg) **39** (10), 1844 (1997) [Phys. Solid State **39** (10), 1647 (1997)].
18. K. S. Aleksandrov, A. T. Anistratov, B. V. Beznosikov, and N. V. Fedoseeva, *Phase Transitions in Crystals of ABX_3 Halides* (Nauka, Novosibirsk, 1981) [in Russian].
19. I. N. Flerov, M. V. Gorev, K. S. Aleksandrov, A. Tressaud, and V. D. Fokina, Kristallografiya **49** (1), 107 (2004) [Crystallogr. Rep. **49** (1), 100 (2004)].
20. I. N. Flerov, M. V. Gorev, V. N. Voronov, and A. F. Bovina, Fiz. Tverd. Tela (St. Petersburg) **38** (7), 2203 (1996) [Phys. Solid State **38** (7), 1213 (1996)].
21. A. A. Udovenko and N. M. Laptash, Acta Crystallogr., Sect. B: Struct. Sci. **64**, 305 (2008).
22. A. A. Udovenko, N. M. Laptash, and I. G. Maslennikova, J. Fluorine Chem. **124**, 5 (2003).
23. M. V. Gorev, I. N. Flerov, E. V. Bogdanov, V. N. Voronov, and N. M. Lapatsh, Fiz. Tverd. Tela (St. Petersburg) **52** (2), 351 (2010) [Phys. Solid State **52** (2), 377 (2010)].
24. A. M. Tishin and Y. I. Spichkin, *The Magnetocaloric Effect and Its Applications* (Institute of Physics, Bristol, 2003).
25. A. S. Mischenko, Q. Zhang, J. F. Scott, R. W. Whatmore, and N. D. Mathur, Science (Washington) **311**, 1270 (2006).

Translated by Yu. Ryzhkov